Nanoscale Research Letters
a SpringerOpen Journal

NANO EXPRESS Open Access

Ferromagnetism and optical properties of $La_{1-x}Al_xFeO_3$ nanopowders

Yutana Janbutrach[1], Sitchai Hunpratub[1] and Ekaphan Swatsitang[2,3*]

Abstract

$La_{1-x}Al_xFeO_3$ ($x = 0.0$, 0.05, 0.1, 0.2, 0.3, 0.4, and 0.5) nanopowders were prepared by polymerization complex method. All prepared samples were characterized by X-ray diffraction (XRD), scanning electron microscopy (SEM), transmission electron microscopy (TEM), Fourier transform infrared spectroscopy (FT-IR), and UV-vis spectrophotometry (UV-vis). The magnetic properties were investigated using a vibrating sample magnetometer (VSM). The X-ray results of all samples show the formation of an orthorhombic phase with the second phase of α-Fe_2O_3 in doped samples. The crystallite sizes of nanoparticles decreased with increasing Al content, and they are found to be in the range of 58.45 ± 5.90 to 15.58 ± 4.64 nm. SEM and TEM images show the agglomeration of nanoparticles with average particle size in the range of 60 to 75 nm. The FT-IR spectra confirm the presence of metal oxygen bonds of O-Fe-O and Fe-O in the FeO_6 octahedra. The UV-vis spectra show strong absorption peaks at approximately 285 nm, and the calculated optical band gaps are found to be in the range of 2.05 to 2.09 eV with increasing Al content. The M-H loop of the pure sample is antiferromagnetic, whereas those of the doped samples tend to be ferromagnetic with increasing Al content. The magnetization, remanent magnetization, and coercive field of the Al-doped sample with $x = 0.5$ are enhanced to 1.665 emu/g, 0.623 emu/g, and 4,087.0 Oe, respectively.

Keywords: Ferromagnetism; Optical properties; Polymerization complex method; $La_{1-x}Al_xFeO_3$; Nanopowders

Background

$LaFeO_3$ with an orthorhombic phase of the ABO_3-type perovskite structure has become a currently attractive research topic because it is proposed for various applications in several advanced technologies such as catalysts [1-3], various kinds of chemical and gas sensors [4-9], and electrode materials in solid oxide fuel cells [10]. In general, $LaFeO_3$ consists of FeO_6 octahedral units with La^{3+} ions at the corners [11,12]. The advantage of this structure is the replaceability of metallic ions at both A and B sites by various transition metals. Pure and doped $LaFeO_3$ (Pd, Al, Zn, Ag, Sr, Ir, Ca, Co, etc.) were studied for various purposes and aspects with reports of optical, electrical, and magnetic properties [13-25].

Research on pure and doped $LaFeO_3$ nanostructures reveal that the property and quality of the materials are strongly influenced by the synthesis method. The synthesis method is usually related to the specific preparation conditions which can result in various properties of the end products. Various techniques were employed for the synthesis of pure and doped $LaFeO_3$ such as sol-gel/combustion method [26-40], microwave-assisted method [41-43], solid-state reaction method [14,44-46], thermal decomposition [47,48], microemulsion method [49], hydrothermal method [50-52], hot soap method [53], spray drying [54], electrospinning [55], drip pyrolysis [19], and polymerization complex method [56-59]. However, polymerization complex method based on polyesterification between citric acid (CA) and ethylene glycol (EG) is the most attractive because it is simple, cost effective, time saving, and environmentally benign.

Thus, we propose in this research the synthesis of $La_{1-x}Al_xFeO_3$ ($x = 0$, 0.05, 0.1, 0.2, 0.3, 0.4, and 0.5) nanopowders using a simple polymerization complex method. The magnetic and optical properties of the products were studied. The magnetization, coercive field, and remanent magnetization are measured, and they are expected to be enhanced due to the substitution of small-radius ions of Al on the La site.

* Correspondence: ekaphan@kku.ac.th
[2]Integrated Nanotechnology Research Center and Department of Physics, Faculty of Science, Khon Kaen University, Khon Kaen 40002, Thailand
[3]Nanotec-KKU Center of Excellence on Advanced Nanomaterials for Energy Production and Storage, Khon Kaen 40002, Thailand
Full list of author information is available at the end of the article

Springer

© 2014 Janbutrach et al.; licensee Springer. This is an Open Access article distributed under the terms of the Creative Commons Attribution License (http://creativecommons.org/licenses/by/4.0), which permits unrestricted use, distribution, and reproduction in any medium, provided the original work is properly credited.

Methods

$La_{1-x}Al_xFeO_3$ ($x = 0$, 0.05, 0.1, 0.2, 0.3, 0.4, and 0.5) were synthesized by polymerization complex method. Stoichiometric amounts of iron nitrate ($Fe(NO_3)_3.9H_2O$, Kanto Chemical Co., Chuo-ku, Japan, 99.9%), lanthanum nitrate ($LaN_3O_9.6H_2O$, Fluka, Seelze, Germany, 99.0%), and aluminum nitrate ($Al(NO_3)_3.9H_2O$, Carlo Erba Reagenti, Milan, Italy, 99.0%) in the ratio of $1 - x$:x:1 (La:Al:Fe) with 1 g of citric acid ($C_6H_8O_7.H_2O$, VWR International Ltd., Radnor, PA, USA, 99.7%) were dissolved in 40 mL ethylene glycol and 20 mL deionized (DI) water. The mixture was magnetically stirred for 1 h in order to obtain stable metal-citric acid complexes. The obtained solution was continuously stirred at 70°C for 1 h. This solution was dried at 120°C on a hot plate. The obtained powders were pre-calcined at 400°C for 3 h to burn out the polymer. The pre-calcined powders were ground and further calcined at 900°C for 3 h in air.

The calcined powders were characterized using an X-ray diffractometer (XRD; XRD-6100, Shimadzu, Kyoto, Japan) with CuKα_1 radiation ($\lambda = 1.5405$ Å). The morphologies of the synthesized products were observed using a scanning electron microscope (SEM; 1450VP, LEO, Hurley, UK) and a transmission electron microscope (TEM; Tecnai G2 20, FEI, Hillsboro, OR, USA). The components of the powders were analyzed by energy-dispersive X-ray spectroscopy (EDX; Tecnai G2 20, FEI). Fourier transform infrared spectroscopy (FT-IR; Spectrum One FT-IR, Perkin Elmer Instrument, Waltham, MA, USA) was employed to investigate functional groups in all samples. The optical properties were studied by ultraviolet-visible spectroscopy (UV-vis; UV-3101PC, Shimadzu). The magnetizations of all samples were measured using a vibrating sample magnetometer (VSM; VersaLab™ Cryogen-free, Quantum Design, San Diego, CA, USA).

Results and discussion

XRD analysis

The XRD patterns of $La_{1-x}Al_xFeO_3$ ($x = 0$, 0.05, 0.1, 0.2, 0.3, 0.4, and 0.5) nanopowders are shown in Figure 1. The results indicate that the products are a perovskite oxide of an orthorhombic structure with the second phase of α-Fe_2O_3 in the doped samples of $x = 0.2$ to 0.5. The XRD results are in good agreement with the standard data of $LaFeO_3$ (JCPDS card no: 37-1493) and α-Fe_2O_3 (JCPDS card no: 89-0595). The average crystallite size is determined from the X-ray line broadening of the (101), (121), (220), (202), (240), (242), and (204) diffraction peaks using the Scherrer equation, and it is found to be decreased with increasing Al content, as summarized in Table 1. The lattice parameters a, b, and c of the doped samples decreased with the increase of Al content due to the replacement of the larger La^{3+} ion (radius approximately 1.36 Å) by a smaller Al^{3+} ion (radius approximately 0.535 Å) [22], as summarized in Table 1. The significant change in the decrease of lattice parameters with increasing Al content is confirmed by the shift of the diffraction peaks to a higher diffraction angle. On the other hand, Al^{3+} ions can be substituted on B sites of Fe^{3+} ions because the ionic radius of Al^{3+} is close to that of the Fe^{3+} ion (radius approximately 0.78 Å), resulting in the formation of the impurity phase of α-Fe_2O_3.

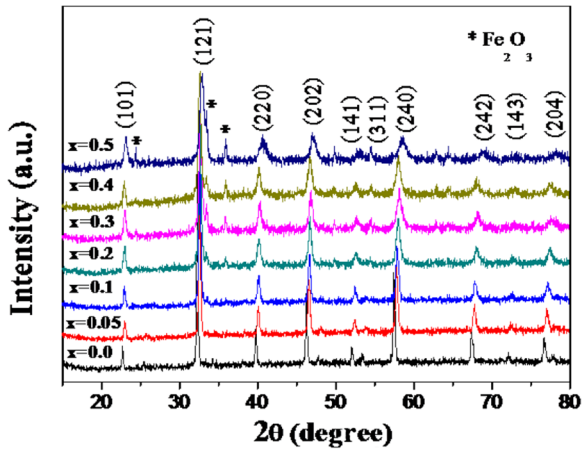

Figure 1 XRD patterns of $La_{1-x}Al_xFeO_3$ ($x = 0.0$, 0.05, 0.1, 0.2, 0.3, 0.4, and 0.5) nanopowders.

SEM analysis

The SEM micrographs of $La_{1-x}Al_xFeO_3$ ($x = 0.0$, 0.1, 0.3, and 0.5) nanopowders are shown in Figure 2. In Figure 2a, the powders are almost irregularly nanoagglomerated with a mean size of approximately 60 to 75 nm. In Figure 2b,c,d, agglomeration of nanoparticles with a size larger than 100 nm and grain growth can be observed in doped samples. Moreover, the SEM images reveal a uniform grain size distribution and homogeneous nanostructure.

Table 1 Lattice parameter and crystallite size of $La_{1-x}Al_xFeO_3$ nanopowders

$La_{1-x}Al_xFeO_3$	Lattice parameter (Å)			Average crystallite size (Å)
	a	*b*	*c*	
$x = 0.0$	5.559	7.862	5.560	58.45 ± 5.90
$x = 0.05$	5.544	7.848	5.549	39.00 ± 1.03
$x = 0.1$	5.536	7.834	5.539	29.83 ± 7.84
$x = 0.2$	5.503	7.812	5.522	24.30 ± 3.76
$x = 0.3$	5.503	7.790	5.506	23.23 ± 5.22
$x = 0.4$	5.506	7.785	5.509	22.35 ± 4.77
$x = 0.5$	5.443	7.762	5.502	15.58 ± 4.64

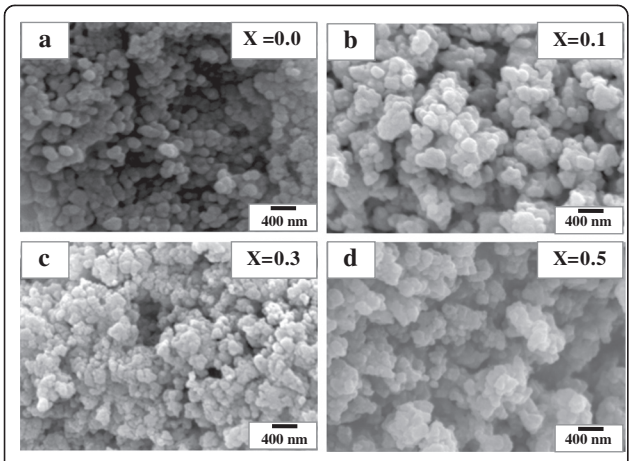

Figure 2 SEM micrographs of $La_{1-x}Al_xFeO_3$ nanopowders. **(a)** $x = 0.0$. **(b)** $x = 0.1$. **(c)** $x = 0.3$. **(d)** $x = 0.5$.

TEM analysis

Figure 3a,b,c,d shows bright-field TEM images with the corresponding selected area electron diffraction (SAED) patterns and EDX spectra of $La_{1-x}Al_xFeO_3$ ($x = 0.0$, 0.1, 0.3, and 0.5) nanopowders. It is obvious in Figure 3a1, b1,c1,d1 that the particulates consist of the agglomeration of numerous nanocrystallite particles of irregular shape, corresponding to the SEM observation in Figure 2. The average particle size is estimated and found to be approximately 60 to 75 nm. The SAED patterns in Figure 3a2,b2,c2,d2 show ring patterns, indicating that all doped samples are polycrystalline. Each SAED pattern can be indexed to a certain crystalline plane which is found to be consistent with that of the XRD results in Figure 1. The EDX spectra of these samples are shown in Figure 3a3,b3,c3,d3. The EDX results clearly show that all samples contain La, Fe, Al, and O with higher intensity peaks of Al in samples of high Al content. The Cu peaks that appeared come from the copper grid.

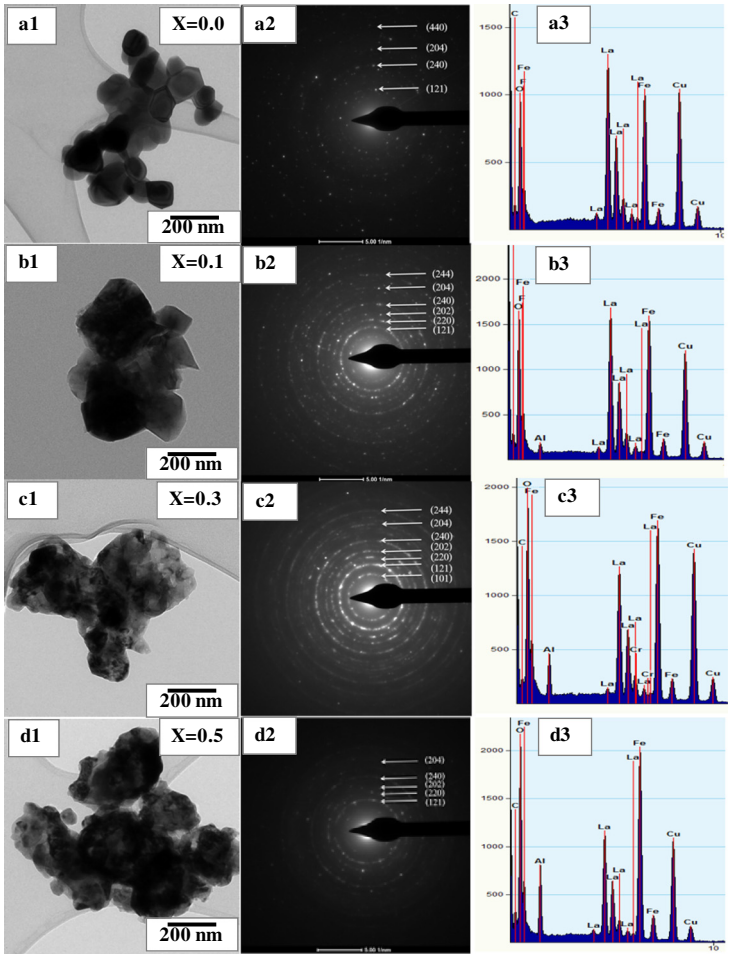

Figure 3 Bright-field TEM images (a1-d1) with the corresponding SAED patterns (a2-d2) and EDX spectra (a3-d3) of $La_{1-x}Al_xFeO_3$ nanopowders. **(a)** $x = 0.0$. **(b)** $x = 0.1$. **(c)** $x = 0.3$. **(d)** $x = 0.5$.

FT-IR analysis

Figure 4 shows the FT-IR spectra of $La_{1-x}Al_xFeO_3$ ($x = 0$, 0.05, 0.1, 0.2, 0.3, 0.4, and 0.5) nanopowders. All spectra show broad absorption peaks at approximately 3,449.13 cm^{-1}, corresponding to the symmetric and asymmetric stretching modes of water molecules. The observed broad band at approximately 1,600 cm^{-1} corresponds to the bending mode of O-H bond. The strong absorption peaks in the range of 500 to 600 cm^{-1} reveal the presence of metal oxygen bonds which can be assigned to the vibrations of Fe-O and O-Fe-O bonding in the octahedral structure of $La_{1-x}Al_xFeO_3$. These results are in good agreement with the FT-IR spectra of pure and doped $LaFeO_3$ reported in the literature [14,41,43,47,50].

UV-vis analysis

The UV-vis spectra of $La_{1-x}Al_xFeO_3$ ($x = 0$, 0.05, 0.1, 0.2, 0.3, 0.4, and 0.5) nanopowders are shown in Figure 5. In Figure 5, broad absorption peaks are observed in all samples at approximately 285 nm with the infinitesimal redshifted to approximately 290 nm. From the plot of $(\alpha hv)^2$ vs. hv in Figure 6a,b,c,d, the optical band gaps (E_g) of the samples can be determined by extrapolating the slope to the zero value of $(\alpha hv)^2$, and the obtained values are summarized in Table 2. It is found that the optical band gaps do not significantly vary with increasing Al content.

VSM analysis

Figure 7a,b,c,d,e,f,g shows the magnetization curves of $La_{1-x}Al_xFeO_3$ ($x = 0$, 0.05, 0.1, 0.2, 0.3, 0.4, and 0.5) nanopowders measured at room temperature by VSM. As can be seen in Figure 7a, the magnetization curve of the pure sample is very narrow, indicating the antiferromagnetic behavior of the sample, while those of the doped samples show larger loops of ferromagnetic behavior with higher magnetization according to higher Al content (Figure 7b,c,d,e,f,g). In addition, the values of coercive field (H_c), magnetization (M), and remanent magnetization (M_r) are enhanced with increasing Al content, as summarized in Table 2. In general, it is well known that pure $LaFeO_3$ exhibits antiferromagnetic behavior. This behavior is due to the anti-alignment of the magnetic moments of the Fe^{3+} ions. However, $LaFeO_3$ can behave ferromagnetically due to the small crystallite size. The decrease of crystallite size can increase the uncompensated spins at the surface [60,61]. In our work, it is evident in Table 1 that the crystallite size of $La_{1-x}Al_xFeO_3$ decreases for higher Al content, resulting in the enhancement of ferromagnetism with higher M value. In addition, the second phase of α-Fe_2O_3 detected in the

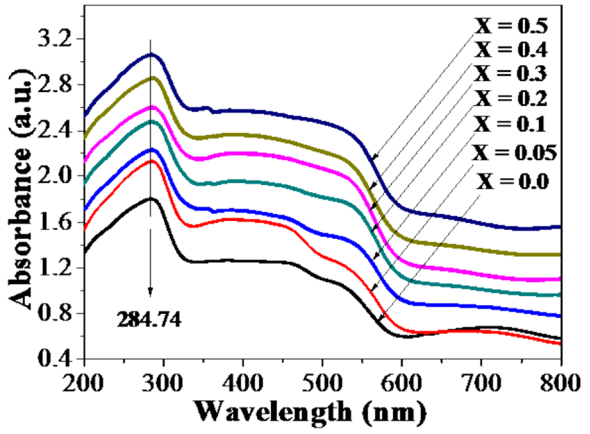

Figure 5 UV-vis spectra of $La_{1-x}Al_xFeO_3$ ($x = 0.0$, 0.05, 0.1, 0.2, 0.3, 0.4, and 0.5) nanopowders.

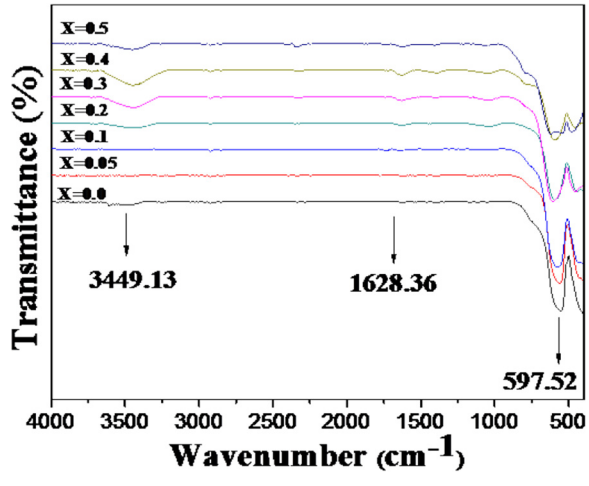

Figure 4 FT-IR spectra of $La_{1-x}Al_xFeO_3$ ($x = 0.0$, 0.05, 0.1, 0.2, 0.3, 0.4, and 0.5) nanopowders.

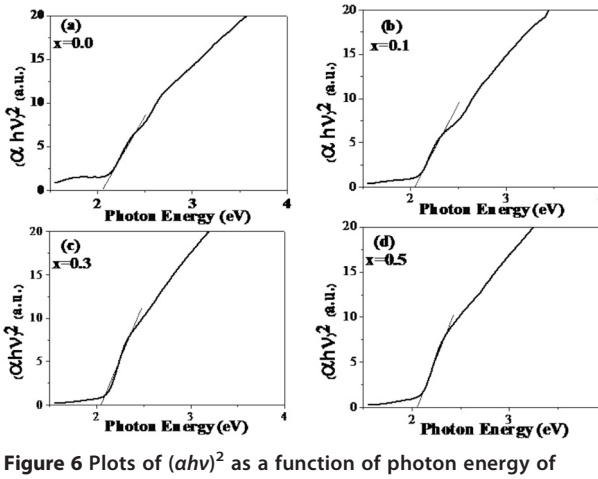

Figure 6 Plots of $(ahv)^2$ as a function of photon energy of $La_{1-x}Al_xFeO_3$ nanopowders. (a) $x = 0.0$. **(b)** $x = 0.1$. **(c)** $x = 0.3$. **(d)** $x = 0.5$.

Table 2 Coercive field (H_c), magnetization (M), remanent magnetization (M_r), and optical band gap (E_g) of $La_{1-x}Al_xFeO_3$ nanopowders

$La_{1-x}Al_xFeO_3$	H_c (Oe)	M (emu/g)	M_r (emu/g)	E_g (eV)
$x = 0.0$	366.8	0.202	0.007	2.05
$x = 0.05$	591.2	0.291	0.008	2.07
x = 0.1	1,597.2	0.196	0.012	2.07
$x = 0.2$	3,390.6	0.300	0.038	2.07
$x = 0.3$	5,308.4	0.509	0.158	2.09
$x = 0.4$	4,399.3	0.899	0.301	2.09
$x = 0.5$	4,087.0	1.665	0.623	2.07

XRD measurements may also be attributed to the ferromagnetism in $La_{1-x}Al_xFeO_3$. Figure 8 shows the temperature-dependent magnetization of $La_{0.5}Al_{0.5}FeO_3$ nanopowder investigated by field-cooled (FC) measurement in the temperature range of 50 to 390 K. The M decreases as the temperature increases because of the thermal fluctuations causing the randomization of polarization direction. It is clearly seen in Figure 8 that the zero value of magnetization cannot be observed in the temperature range of measurement, implying that the Curie temperature (T_c) is above 400 K.

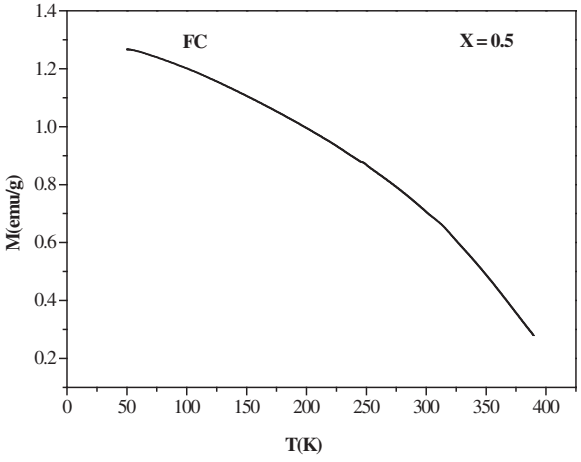

Figure 8 Magnetization of $La_{0.5}Al_{0.5}FeO_3$ nanopowder as a function of temperature measured by field cooling process.

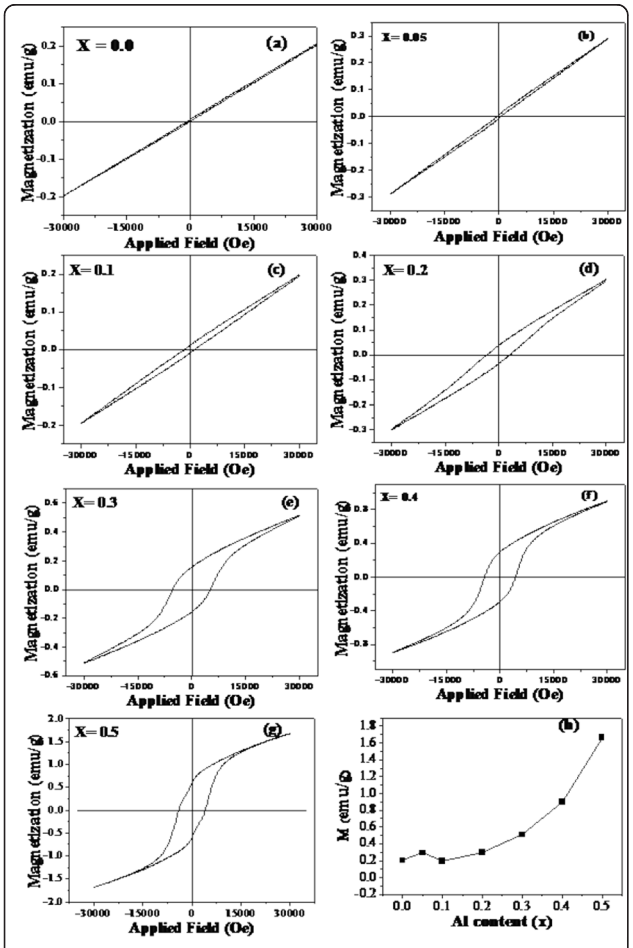

Figure 7 Magnetization measurements at room temperature of $La_{1-x}Al_xFeO_3$ nanopowders. (a) $x = 0.0$. **(b)** $x = 0.05$. **(c)** $x = 0.1$. **(d)** $x = 0.2$. **(e)** $x = 0.3$. **(f)** $x = 0.4$. **(g)** $x = 0.5$. **(h)** M as a function of Al content.

Conclusions

In summary, $La_{1-x}Al_xFeO_3$ ($x = 0$, 0.05, 0.1, 0.2, 0.3, 0.4, and 0.5) nanopowders were successfully synthesized by polymerization complex method at a temperature of 900°C for 3 h in air. XRD analysis reveals an orthorhombic phase of the nanopowders with average crystallite size in the range of 15.58 ± 4.64 to 58.54 ± 5.90 nm. The impurity phase of α-Fe_2O_3 is found in doped samples of $x \geq 0.2$. SEM and TEM images show agglomerated nanoparticles of irregular shape with estimated particle sizes in the range of 60 to 75 nm. The lattice parameters are found to decrease with increasing Al content. The EDX results clearly show only the main peaks of La, Fe, Al, and O in all samples. The UV-vis spectra show the infinitesimal shift from 285 to 290 nm as the Al content is increased. The increase of Al content does not significantly affect the optical band gaps which are found to be in the range of 2.05 to 2.09 eV. Al^{3+} substitution in $LaFeO_3$ crystals can enhance the magnetization (M), coercive field (H_c), and remanent magnetization (M_r) of Al-doped samples by a factor of 8, 11, and 89, respectively. The ferromagnetism in $La_{1-x}Al_xFeO_3$ is due to the size effect and impurity.

Competing interests

The authors declare that they have no competing interests.

Authors' contributions

YJ designed and carried out all the experiments and data analysis and participated in preparing the draft of the manuscript. SH co-supervised the research and gave discussion. ES, the project coordinator, supervised the

research, designed the experiment, participated in preparing the draft of the manuscript, and revised the manuscript. All authors read and approved the final manuscript.

Acknowledgements
The authors would like to thank the Department of Physics of the Faculty of Science, Ubon Ratchathani University for providing the XRD facility and Khon Kaen University for providing the SEM, TEM, FT-IR, UV-vis, and VSM facilities. This work is partially supported by the Nanotec-KKU Center of Excellence on Advanced Nanomaterials for Energy Production and Storage and the Integrated Nanotechnology Research Center and Department of Physics, Faculty of Science, Khon Kaen University.

Author details
[1]Materials Science and Nanotechnology Program, Faculty of Science, Khon Kaen University, Khon Kaen 40002, Thailand. [2]Integrated Nanotechnology Research Center and Department of Physics, Faculty of Science, Khon Kaen University, Khon Kaen 40002, Thailand. [3]Nanotec-KKU Center of Excellence on Advanced Nanomaterials for Energy Production and Storage, Khon Kaen 40002, Thailand.

Received: 16 July 2014 Accepted: 21 August 2014
Published: 15 September 2014

References

1. Mawdsley JR, Krause TR: **Rare earth-first-row transition metal perovskites as catalysts for the autothermal reforming of hydrocarbon fuels to generate hydrogen.** *Appl Catal A-Gen* 2008, **334**(1–2):311–320.
2. Pecchi G, Reyes P, Zamora R, Cadus LE, Fierro JLG: **Surface properties and performance for VOCs combustion of $LaFe_{1-y}Ni_yO_3$ perovskite oxides.** *J Solid State Chem* 2008, **181**(4):905–912.
3. Delmastro A, Mazza D, Ronchetti S, Vallino M, Spinicci R, Brovetto P, Salis M: **Synthesis and characterization of non-stoichiometric $LaFeO_3$ perovskite.** *Mater Sci Eng B* 2001, **79:**140–145.
4. Toan NN, Saukko S, Lantto V: **Gas sensing with semiconducting perovskite oxide $LaFeO_3$.** *Physica B* 2003, **327:**279–282.
5. Lantto V, Saukko S, Toan NN, Reyes LL, Granqvist CG: **Gas sensing with perovskite-like oxides having ABO_3 and BO_3 structures.** *J Electroceram* 2004, **13:**721–726.
6. Martinelli G, Carotta M, Ferroni M, Sadaoka Y, Traversa E: **Screen-printed perovskite-type thick films as gas sensors for environmental monitoring.** *Sensor Actuat B-chem* 1999, **55:**99–110.
7. Inoue T, Seki N, Eguchi K, Arai H: **Low-temperature operation of solid electrolyte oxygen sensors using perovskite-type oxide electrodes and cathodic reaction kinetics.** *J Electrochem Soc* 1990, **137:**2523.
8. Alcock CB, Doshi RC, Shea Y: **Perovskite electrodes for sensors.** *Solid State Ionics* 1992, **51:**281.
9. Zhao J, Liu Y, Li X, Lu G, You L, Liang X, Liu F, Zhang T, Du Y: **Highly sensitive humidity sensor based on high surface area mesoporous $LaFeO_3$ prepared by a nanocasting route.** *Sensor Actuat B Chem* 2013, **18:**802–809.
10. Minh NQ: **Ceramic fuel cells.** *J Am Ceram Soc* 1993, **76:**563–588.
11. Fossdal A, Menon M, Warnhus I, Wiik K, Einarsrud M, Grande T: **Crystal structure and thermal expansion of $La_{1-x}Sr_xFeO_3$ materials.** *J Am Ceram Soc* 2004, **87:**1952–1958.
12. Bellakki MB, Manivannan V, McCurdy P, Kohli S: **Synthesis, and measurement of structural and magnetic properties, of $La_{1-x}Na_xFeO_3$ $(0.0 \le x \le 0.3)$ perovskite oxides.** *J Rare Earth* 2009, **27:**691–697.
13. Yao T, Ariyoshi A, Inui T: **Synthesis of $LaMeO_3$ (Me = Cr, Mn, Fe, Co) perovskite oxides from aqueous solutions.** *J Am Ceram Soc* 1997, **80**(9):2441.
14. Kaiwen Z, Xuehang W, Wenwei W, Jun X, Siqi T, Sen L: **Nanocrystalline $LaFeO_3$ preparation and thermal process of precursor.** *Adv Powder Technol* 2013, **24:**359–363.
15. Eyssler A, Winkler A, Mandaliev P, Hug P, Weidenkaff A, Ferri D: **Influence of thermally induced structural changes of 2 wt% Pd/$LaFeO_3$ on methane combustion activity.** *Appl Catal B-Environ* 2011, **106:**494–502.
16. Ahmed MA, Okasha N, Hussein B: **Enhancement of the magnetic properties of Al/La multiferroic.** *J Magn Magn Mater* 2012, **324:**2349–2354.
17. Bhat I, Husain S, Khan W, Patil SI: **Effect of Zn doping on structural, magnetic and dielectric properties of $LaFeO_3$ synthesized through sol–gel auto-combustion process.** *Mater Res Bull* 2013, **48:**4506–4512.
18. Desai PA, Athawale AA: **Microwave combustion synthesis of silver doped lanthanum ferrite magnetic nanoparticles.** *Defence Sci J* 2013, **63:**285–291.
19. Kindermann L, Das D, Bahadur D, Nickel H, Hilpert K: **Influence of iridium on the reactivity of $LaFeO_3$ base perovskites.** *Solid State Ionics* 1998, **106:**165–172.
20. Li F, Liu Y, Liu R, Sun Z, Zhao D, Kou C: **Preparation of Ca-doped $LaFeO_3$ nanopowders in a reverse microemulsion and their visible light photocatalytic activity.** *Mater Lett* 2010, **64:**223–225.
21. Haron W, Thaweechai T, Wattanathana W, Laobuthee A, Manaspiya H, Veranitisagul C, Koonsaeng N: **Structural characteristics and dielectric properties of $La_{1-x}Co_xFeO_3$ and $LaFe_{1-x}Co_xO_3$ synthesized via metal organic complexes.** *Energy Procedia* 2013, **34:**791–800.
22. Acharya S, Deb AK, Das D, Chakrabarti PK: **Enhanced magnetic behavior of Al substituted $LaFeO_3$ ($La_{(1-x)}Al_xFeO_3$, $x = 0.10$ and 0.30).** *Mater Lett* 2011, **65:**1280–1282.
23. Ahmed MA, El-Dek SI: **Extraordinary role of Ca^{2+} ions on the magnetization of $LaFeO_3$ orthoferrite.** *Mater Sci Eng B* 2006, **128:**30–33.
24. Isupova LA, Yakovleva IS, Tsybulya SV, Kryukova GN, Boldyreva NN, Vlasov AA, Alikina GM, Ivanov VP, Sadykov VA: **Physicochemical and catalytic properties of $La_{1-x}Ca_x$ $FeO_{3-0.5x}$ perovskites.** *Kinet Catal* 2000, **41:**287–291.
25. Traversa E, Nunziante P, Sangaletti L, Allieri B, Depero LE, Aono H, Sadaoka Y: **Synthesis and structural characterization of trimetallic perovskite-type rare-earth orthoferrites, $La_xSm_{1-x}FeO_3$.** *J Am Ceram Soc* 2000, **83**(5):1087.
26. Köferstein R, Jäger L, Ebbinghaus SG: **Magnetic and optical investigations on $LaFeO_3$ powders with different particle sizes and corresponding ceramics.** *Solid State Ionics* 2013, **249–250:**1–5.
27. Bellakki MB, Kelly BJ, Manivannan V: **Synthesis, characterization, and property studies of (La, Ag)FeO_3 $(0.0 \le x \le 0.3)$ perovskites.** *J Alloy Compd* 2010, **489:**64–71.
28. Feng J, Liu T, Xu Y, Zhao J, He Y: **Effects of PVA content on the synthesis of $LaFeO_3$ via sol–gel route.** *Ceram Inter* 2011, **37:**1203–1207.
29. Qi X, Zhou J, Yue Z, Gui Z, Li L: **A simple way to prepare nanosized $LaFeO_3$ powders at room temperature.** *Ceram Inter* 2003, **29:**347–349.
30. Parida KM, Reddy KH, Martha S, Das DP, Biswal N: **Fabrication of nanocrystalline LaFeO3: an efficient sol–gel auto-combustion assisted visible light responsive photocatalyst for water decomposition.** *Int J Hydrogen Energy* 2010, **35:**12161–12168.
31. Liu T, Xu Y: **Synthesis of nanocrystalline $LaFeO_3$ powders via glucose sol–gel route.** *Mater Chem Phys* 2011, **129:**1047–1050.
32. Qi X, Zhou J, Yue Z, Gui Z, Li L: **Auto-combustion synthesis of nanocrystalline $LaFeO_3$.** *Mater Chem Phys* 2002, **78:**25–29.
33. Shabbir G, Qureshi AH, Saeed K: **Nano-crystalline $LaFeO_3$ powders synthesized by the citrate–gel method.** *Mater Lett* 2006, **60:**3706–3709.
34. Tijare SN, Joshi MV, Padole PS, Mangrulkar PA, Rayalu SS, Labhsetwar NK: **Photocatalytic hydrogen generation through water splitting on nano crystalline $LaFeO_3$ perovskite.** *Int J Hydrogen Energy* 2012, **37:**10451–10456.
35. Li F, Liu Y, Sun Z, Liu R, Kou C, Zhao Y, Zhao D: **Facile preparation of porous $LaFeO_3$ nanomaterial by self-combustion of ionic liquids.** *Mater Lett* 2011, **65:**406–408.
36. Jadhav AD, Gaikwad AB, Samuel V, Ravi V: **A low temperature route to prepare $LaFeO_3$ and $LaCoO_3$.** *Mater Lett* 2007, **61:**2030–2032.
37. Wang Y, Zhu J, Zhang L, Yang X, Lu L, Wang X: **Preparation and characterization of perovskite $LaFeO_3$ nanocrystals.** *Mater Lett* 2006, **60:**1767–1770.
38. Zhong Z, Chen K, Ji Y, Yan Q: **Methane combustion over B-site partially substituted perovskite-type $LaFeO_3$ prepared by sol–gel method.** *Appl Catal A* 1997, **156:**2941.
39. Cho YG, Choi KH, Kim RY, Jung JS, Lee SH: **Characterization and catalytic properties of surface La-rich $LaFeO_3$ perovskite.** *Bull Korean Chem Soc* 2009, **30:**6.
40. Kondakindi RR, Karan K, Peppley BA: **A simple and efficient preparation of $LaFeO_3$ nanopowders by glycine–nitrate process: effect of glycine concentration.** *Ceram Inter* 2012, **38:**449–456.
41. Tang P, Tong Y, Chen H, Cao F, Pan G: **Microwave-assisted synthesis of nanoparticulate perovskite $LaFeO_3$ as a high active visible-light photocatalyst.** *Curr Appl Phys* 2013, **13:**340–343.
42. Farhadi S, Momeni Z, Taherimehr M: **Rapid synthesis of perovskite-type $LaFeO_3$ nanoparticles by microwave-assisted decomposition of bimetallic La[Fe(CN)$_6$] 5H$_2$O compound.** *J Alloy Compd* 2009, **471:**15–18.
43. Ding JLX, Shu H, Xie J, Zhang H: **Microwave-assisted synthesis of perovskite $ReFeO_3$ (Re: La, Sm, Eu, Gd) photocatalyst.** *Mater Sci Eng B* 2010, **171:**31–34.

44. Chu X, Zhou S, Zhang W, Shui H: **Trimethylamine sensing properties of nano-$LaFeO_3$ prepared using solid-state reaction in the presence of PEG400.** *Mater Sci Eng B* 2009, **164:**65–69.
45. Idrees M, Nadeem M, Atif M, Siddique M, Mehmood M, Hassan MM: **Phase structure, microstructure and dielectric properties of $(K_{0.5}Na_{0.5})NbO_3$-$LaFeO_3$ high-temperature dielectric ceramics.** *Acta Mater* 2011, **59:**1338–1345.
46. Ivanov SA, Tellgren R, Porcher F, Ericsson T, Mosunov A, Beran P, Korchagina SK, Anil Kumar P, Mathieu R, Nordblad P: **Preparation, structural, dielectric and magnetic properties of $LaFeO_3$–$PbTiO_3$ solid solutions.** *Mater Res Bull* 2012, **47:**3253–3268.
47. Wei ZX, Xu YQ, Liu HY, Hu CW: **Preparation and catalytic activities of $LaFeO_3$ and Fe_2O_3 for HMX thermal decomposition.** *J Hazard Mater* 2009, **165:**1056–1061.
48. Sadaoka Y, Aonoa H, Traversa E, Sakamoto M: **Thermal evolution of nanosized $LaFeO_3$ powders from a heteronuclear complex, $La[Fe(CN)_6]$ nH_2O.** *J Alloy Compd* 1998, **278:**135–141.
49. Giannakas AE, Ladavos AK, Pomonis PJ: **Preparation, characterization and investigation of catalytic activity for NO + CO reaction of $LaMnO_3$ and $LaFeO_3$ perovskites prepared via microemulsion method.** *Appl Catal B-Environ* 2004, **49:**147–158.
50. Thirumalairajan S, Girija K, Ganesh I, Mangalaraj D, Viswanathan C, Balamurugan A, Ponpandian N: **Controlled synthesis of perovskite $LaFeO_3$ microsphere composed of nanoparticles via self-assembly process and their associated photocatalytic activity.** *Chem Eng J* 2012, **209:**420–428.
51. Zheng W, Liu R, Peng D, Meng G: **Hydrothermal synthesis of $LaFeO_3$ under carbonate-containing medium.** *Mater Lett* 2000, **43:**19–22.
52. Ji K, Dai H, Deng J, Song L, Xie S, Han W: **Glucose-assisted hydrothermal preparation and catalytic performance of porous $LaFeO_3$ for toluene combustion.** *J Solid State Chem* 2013, **199:**164–170.
53. Fujii T, Matsusue I, Nakatsuka D, Nakanishi M, Takada J: **Synthesis and anomalous magnetic properties of $LaFeO_3$ nanoparticles by hot soap method.** *Mater Chem Phys* 2011, **129:**805–809.
54. Fossdal A, Einarsrud MA, Grande T: **Mechanical properties of $LaFeO_3$ ceramics.** *J Eur Ceram Soc* 2005, **25:**927–933.
55. Lee WY, Yun HJ, Yoon JW: **Characterization and magnetic properties of $LaFeO_3$ nanofibers synthesized by electrospinning.** *J Alloy Compd* 2014, **583:**320–324.
56. Popa M, Moreno JMC: **Lanthanum ferrite ferromagnetic nanocrystallites by a polymeric precursor route.** *J Alloy Compd* 2011, **509:**4108–4116.
57. Liu X, Ji H, Gu Y, Xu M: **Preparation and acetone sensitive characteristics of nano-$LaFeO_3$ semiconductor thin films by polymerization complex method.** *Mater Sci Eng B* 2006, **133:**98–101.
58. Popa M, Frantti J, Kakihana M: **Lanthanum ferrite $LaFeO_{3+d}$ nanopowders obtained by the polymerizable complex method.** *Solid State Ionics* 2002, **154–155:**437–445.
59. Popa M, Frantti J, Kakihana M: **Characterization of $LaMeO_3$ (Me: Mn, Co, Fe) perovskite powders obtained by polymerizable complex method.** *Solid State Ionics* 2002, **154–155:**135–141.
60. Kodama RH, Makhlouf SA, Berkowitz AE: **Finite size effects in antiferromagnetic NiO nanoparticles.** *Phys Rev Lett* 1997, **79:**1393–1396.
61. Winkler E, Zyster RD, Mansilla MV, Fiorant D: **Surface anisotropy effects in NiO nanoparticles.** *Phys Rev B* 2005, **72:**132409.

doi:10.1186/1556-276X-9-498
Cite this article as: Janbutrach *et al.*: **Ferromagnetism and optical properties of $La_{1-x}Al_xFeO_3$ nanopowders.** *Nanoscale Research Letters* 2014 **9**:498.

Submit your manuscript to a SpringerOpen journal and benefit from:

► Convenient online submission
► Rigorous peer review
► Immediate publication on acceptance
► Open access: articles freely available online
► High visibility within the field
► Retaining the copyright to your article

Submit your next manuscript at ► springeropen.com